Electrodeposition and Photocatalytic Selectivity of ZnO/Methyl Blue Hybrid Thin Films

Peng Liu,[†,‡] Weiying Li,*[,†] and Jingbo Zhang*[,‡]

State Key Laboratory of Pollution Control & Resource Reuse, Tongji University, Shanghai 200092, China, and Beijing National Laboratory for Molecular Sciences, Key Laboratory of Photochemistry, Institute of Chemistry, Chinese Academy of Sciences, Beijing 100190, China

Received: April 28, 2009; Revised Manuscript Received: June 11, 2009

ZnO/methyl blue hybrid thin films were successfully electrodeposited from an oxygen-saturated aqueous solution of $ZnCl_2$ containing methyl blue (MB) as a structure-directing agent. The addition of MB promotes the crystal growth of ZnO and thus affects the crystallographic orientation and the surface morphology of the hybrid film. The electrodeposited hybrid thin films show porous morphology and hexagonal wurtzite crystalline structure. After extracting MB by dipping the hybrid film in a dilute base solution, the resulting porous film exhibits satisfied photocatalytic activity to degrade MB and eosin Y (EY). And the photodegradation apparent rate constant for MB is almost 5.5 times higher than that of EY. The high photodegradation selectivity to MB is attributed to the synergetic effect that the porous ZnO film obtained by extracting MB from ZnO/MB hybrid thin film adsorbs MB more favorably than EY. This interesting result could shed some light on the application of this technology for the selective degradation of organic pollutants.

1. Introduction

Nanocrystalline semiconductor ZnO, which has good optical, electrical and piezoelectric properties, has drawn considerable attention due to its extensive applications in areas such as field-emission displays, gas sensors, dye-sensitized solar cells, etc. Generally, a ZnO film can be fabricated by several approaches including metal organic chemical vapor deposition (MOVCD), chemical bath deposition, sputtering, pulsed laser deposition, and electrodeposition.[1−6] Due to the advantages such as being a low cost, simple, low-temperature, and environmentally benign process demonstrated by electrodeposition, this desirable technique is widely applied to the preparation of ZnO nanofilms and other materials.[7−9] Recently, the one-step electrodeposition of the ZnO/organic molecule hybrid thin films by addition of various structure-directing agents has been reported, and the structure-directing agents, such as xanthene dyes,[10] sodium laurylsulfate,[11] and citric acid,[4] can control crystalline orientation and film morphologies to form various porous crystalline ZnO thin films. As a structure-directing agent, it must have negatively charged substituent groups such as carboxylic, sulfonic, or phosphonic acid groups, which anchor directly to the ZnO crystallites formed during electrodeposition to create novel structure and morphology. Because the structure-directing agents actively participate in the electrochemical process, influencing the deposition of ZnO films, as an inorganic/organic hybrid material, they exhibit enhanced or totally new properties due to the combination of ZnO and organic materials at nanometer scale or below. The loaded organic molecules, such as xanthene dyes, can be extracted from the hybrid film electrodeposited at the reduced state of dye by rinsing the film into a dilute base solution to obtain the porous ZnO film.[12] Therefore, the one-step electrodeposition of ZnO/dye hybrid thin films is also considered as a method to prepare porous ZnO thin films, and their morphologies can be controlled by the addition of organic additives.

Until now, much attention has been paid to the application of the resulting porous films on dye sensitized solar cells. ZnO, like TiO_2, is known to be an effective photocatalyst to degrade organic pollutants dissolved in solution.[12] Adsorption of organic pollutants on the photocatalyst surface is a prerequisite for the degradation of pollutants. The adsorption chemistry of dye on the photocatalyst surface such as adsorption structure and chemical stability depends on the surface condition of the porous film, which consequently affects the degradation efficiency. After extraction of dye from the ZnO/dye hybrid thin film, the empty surface should favor adsorption of the same dye used to deposit hybrid film more than other dyes. If so, the resulting ZnO porous film should show a high photocatalystic efficiency to degrade dye used during electrodeposition of the ZnO/dye hybrid thin film, namely, we can find a way to improve photocatalytic selectivity.

In the present work, methyl blue (MB) having three sulfonic groups was used as a structure-directing agent to electrodeposit a series of ZnO/MB hybrid films with different morphologies and crystalline structure by adding different amounts of MB. The effect of addition amounts of MB on the morphology and crystalline structure was discussed. After exaction of MB loaded into the film, the porous ZnO film was used as a photocatalyst to degrade MB and eosin Y (EY). The catalytic selectivity enhancement to degrade MB of porous ZnO films prepared with addition of MB was evaluated.

2. Experimental Section

The electrodeposition of ZnO was carried out in an oxygen-saturated mixed aqueous bath containing 5 mM $ZnCl_2$ (Merck) and 0.1 M KCl with different concentrations of MB (SCR) ranging from 9 to 150 μM serving as structure-directing agents. The transparent conducting glass coated with F-doped tin oxide (FTO, 20 Ω/square, Hake New Energy Co., Ltd.) was used as a substrate for the electrodeposition of ZnO/dye hybrid thin

* To whom correspondence should be addressed. J.Z.: phone 86-10-82615031, fax 86-10-82617315, e-mail jbzhang@iccas.ac.cn.
† Tongji University.
‡ Chinese Academy of Sciences.

10.1021/jp903896j CCC: $40.75
Published on Web 07/02/2009

films. Prior to the deposition process, the FTO glass was ultrasonically cleaned in acetone and ethanol for 15 min, then etched in a 45% nitric acid for 2 min, and finally rinsed with deionized water. The cleaned FTO substrate was fixed to a rotating disk electrode (RDE) with an active diameter of 16 mm (2 cm^2 of geometric area) and the rotation speed was set at 500 rpm. The electrodeposition procedure was performed in a classical three-electrode system with a saturated calomel electrode (SCE) as a reference electrode, a platinum wire as a counter electrode, and the FTO-RDE as a working electrode, respectively. The deposition potential was −1.0 V vs. SCE controlled by a Solartron SI 1287 electrochemical interface system and the deposition bath was maintained at 70 °C with a thermostat. The as-deposited films were rinsed with deionized water and dried in air at room temperature. The amount of dye loaded into the film was determined by completely dissolving a known area of the hybrid film into a known volume of pH 10.5 NaOH aqueous solution and measuring its optical absorbance at the absorption maximum of dye with a spectrophotometer (UV3010, Hitachi).

Fourier-transform infrared spectra (FTIR) measurements of the samples were carried out on a spectrometer (Tensor 27, Bruker). Measurements were performed in the transmission mode in spectroscopic grade KBr pellets with powders scratched from the electrodeposited film. The surface and cross-sectional morphologies of the hybrid film were observed on a scanning electron microscope (SEM, S-4300, S-4800, Hitachi) operated at an acceleration voltage of 15 kV. The crystallographic characterization of the electrodeposited film was determined by an X-ray diffractometer (Riguku D/max 2500) by Cu Kα irradiation.

The photodegradation experiments of MB and EY (Kanto) were conducted in an open beaker with 100 mL capacity at room temperature, and the beaker was open to air to ensure enough oxygen in the solution. For comparison, the ZnO/EY hybrid film was prepared according to the same electrodeposition conditions by adding 50 μM EY other than MB. The porous ZnO films were prepared by extracting dye from ZnO/dye hybrid films. The pure ZnO or porous ZnO film with 2 cm^2 of geometric area was laid at the bottom of the beaker, immersed by 15 mL of aqueous solution containing MB or EY with the initial concentration of 36 μM, which was exposed to illumination of a 125 W high-pressure Hg lamp ($\lambda > 320$ nm). Prior to the irradiation, the solution with ZnO film was placed in darkness for 10 min to establish adsorption−desorption equilibrium. The concentration of dye after adsorption−desorption equilibrium was treated as C_0. The change in the concentration of dye based on C_0 was detected by measuring absorbance of the dye solution taken out regularly from the reactor beaker.

3. Results and Discussion

The addition of water-soluble dye with anchoring groups to the electrodeposition solution can affect the crystal growth during the electrodeposition of ZnO. MB with three sulfonic groups in one molecular structure as shown in Figure 1 was used as a structure-directing agent to be added into deposition solution to electrodeposit ZnO/MB hybrid thin films. The chronoamperograms measured during the electrodeposition of ZnO and ZnO/MB films are presented in Figure 2, and the initial current behavior was enlarged as an inset in Figure 2. In the absence of MB, the cathodic current density increases sharply during the first 15 s and then levels off toward a steady value. When MB is added, the current density grows gradually at the beginning of the electrodeposition and then decreases to a steady

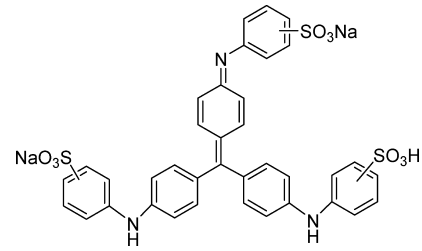

Figure 1. Molecular structure of MB.

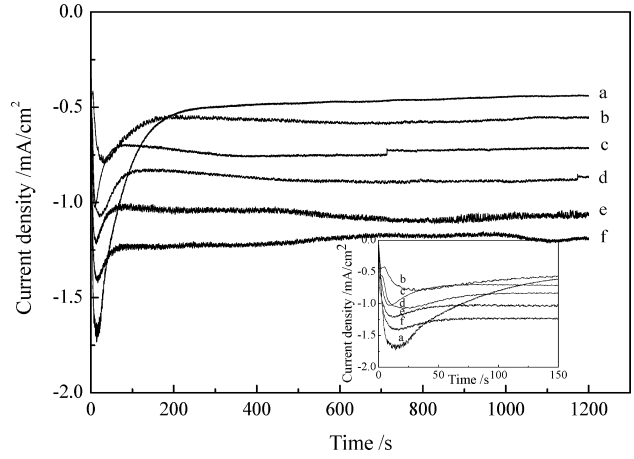

Figure 2. Chronoamperograms measured during the electrodeposition of the hybrid thin films under various MB concentrations of 0 (a), 9 (b), 30 (c), 60 (d), 120 (e), and 150 μM (f).

value creating a current peak. The steady value of current density is enhanced from 0.55 to 1.25 mA cm^{-2} by the addition of MB in deposition solution ranging from 9 to 150 μM, while the shapes of their chronoamperic curves are almost identical. In spite of the presence of dye or not, all the electrodeposition processes go through the same stage that the current density decreases from the maximum value to a relatively small and stable one, and the decreasing extent is comparatively smaller for higher concentrations of dye. As described elsewhere,[13,14] the observed current transient at the beginning of the electrolysis is typical for the initial nucleation and subsequent three-dimensional growth of the seed crystals. When the crystals grow and become larger, they merge together and thus decrease the surface area of ZnO, which leads to a low steady current density. Furthermore, the steady value of current density for ZnO growth with MB is apparently larger than that in the MB-free solution, and it is enhanced with the concentration of added MB, which is demonstrated by the passed charge (Table 1) during the electrolysis calculated from the chronoamperograms. In the previous study on electrodeposition of ZnO/EY thin film from dissolved molecular oxygen precursor, EY was found to catalyze the reduction of oxygen.[15] The catalytic action of EY toward oxygen reduction was observed only when Zn^{2+} ion was present in solution, indicating a high complexity of the catalysis. Similar to these results,[16,17] the current density is greatly enhanced upon increasing the concentration of MB. It is concluded that MB catalyzes the reduction of oxygen and promotes the nucleation as well as the crystal growth of ZnO.

Figure 3 shows the absorption spectra of the ZnO/MB hybrid thin film before and after soaking in dilute NaOH solution. The loaded MB could be completely desorbed from the hybrid film when the film was soaked in dilute base solution. The empty spaces lead to the formation of a highly porous ZnO film. After extracting MB, this porous film could be re-adsorbed by dipping it in MB or EY solution. The loaded MB amount during the

TABLE 1: The Passed Charge, Film Thickness, Amount of MB Loaded into the Film, and Amount of Re-adsorbed MB and EY for the ZnO/MB Hybrid Thin Films Electrodeposited from the Baths Containing Different Concentrations of MB

amount of added MB[a]/μM	passed charge/C cm^{-2}	film thickness/μm	amount of loaded MB/mol cm^{-2}	amount of re-adsorbed MB/mol cm^{-2}	amount of re-adsorbed EY/mol cm^{-2}
0	0.29	0.70		1.71×10^{-8}	1.50×10^{-9}
9	0.34	0.80	2.34×10^{-9}	2.07×10^{-8}	1.80×10^{-9}
30	0.44	0.91	3.90×10^{-9}	3.61×10^{-8}	4.04×10^{-9}
60	0.51	1.15	5.44×10^{-9}	5.79×10^{-8}	5.90×10^{-9}
120	0.64	1.38	4.66×10^{-8}	1.09×10^{-7}	1.03×10^{-8}
150	0.65	1.62	5.52×10^{-8}	1.36×10^{-7}	1.92×10^{-8}

[a] The added amount of MB during electrodeposition of ZnO/MB hybrid thin films.

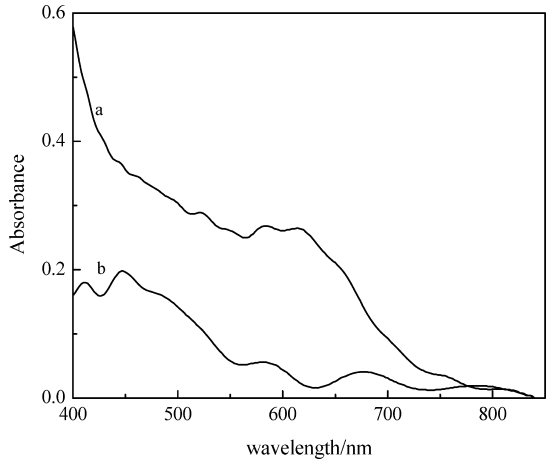

Figure 3. Absorption spectra of the as-deposited hybrid thin film (a) and the film after extracting MB in dilute NaOH solution (b). ZnO/MB hybrid thin film was deposited with 90 μM MB at -1.0 V vs. SCE for 30 min.

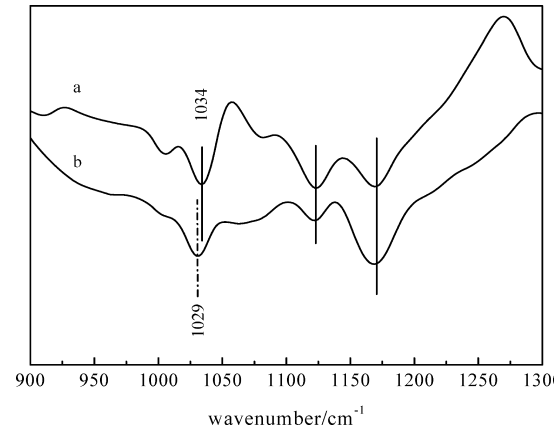

Figure 4. FTIR spectra of pure MB used in this experiment (a) and powder sample scratched from the ZnO/MB hybrid thin film electrodeposited with 150 μM MB (b).

electrolysis and film thickness as well as the re-adsorbed MB and EY amount for the films deposited at various MB concentrations were collected in Table 1. As the added MB amount is increased from 9 to 150 μM, the loaded amount is increased from 2.34×10^{-9} to 5.52×10^{-8} mol cm^{-2} correspondingly. The dye loading increases almost linearly with the dye concentration in electrodeposition solution. At the same time, the film thickness increases almost in the same trend as the increase of MB concentration. So it is reasonable to conclude at this point that MB has a catalytic effect on the growth of the ZnO film.

As already mentioned, the loaded MB could be desorbed from the hybrid film by soaking the film in dilute NaOH solution, while the attempts to desorb MB by dipping the film into water or ethanol fail. This indicates that the MB molecules are located on the surface of ZnO crystals to be accessible by NaOH solution and the dye molecules are not physically occluded by the film but chemically attached to ZnO by a certain chemical bond.[18] Figure 4 shows FTIR spectra of the pure MB and the ZnO/MB powder scratched off from the FTO substrate. For the pure MB, a peak at 1034 cm^{-1}, which is characteristic for the band of S═O, was observed. Whereas compared with FTIR spectra obtained for ZnO/MB hybrid thin film, the band of 1034 cm^{-1} is obviously shifted to a smaller wavenumber of 1029 cm^{-1}. The shifting of the wavenumber upon substitution of Na^+ ion by Zn^{2+} ion suggests electron donation from the sulfonic acid group to zinc.[18] That is to say, this shift is due to the formation of a chemical bond between the sulfonic groups and the ZnO surface.

The deposited ZnO/MB hybrid thin film structure is observed by SEM and shown in Figure 5. The films deposited with various concentrations of MB are obviously different from typical pure ZnO film structure consisting of uniform hexagonal faces.[19] The surface morphology of the ZnO/MB hybrid film obtained by minor addition of 9 μM MB to the deposition bath (Figure 5a) shows that the irregularly connected nanoparticles (typically 40 nm in diameter) randomly stack and form narrow apertures. Its high-magnification SEM image (Figure 5b) clearly evinces that each particle is made up of an aggregation of some small nanoscale crystallites. This kind of highly porous structure can dramatically increase the surface area of ZnO crystals. As the concentration of MB was increased to 30 μM, the surface view (Figure 5c) and cross-section image (insert in Figure 5c) show the presence of vertically aligned ZnO nanopillars with sphere tops. These nanopillars are 30−60 nm in diameter and 700−800 nm in length. The film deposited involving 60 μM MB consists of more tightly arranged and orderly connected nanopillars (Figure 5d), and the presence of apertures cannot be clearly recognized. The interesting phenomena is that 2D wall-like structures grow out of the plane and are found to be randomly distributed on the surface layer of the film. With further increasing MB concentration to 90 μM, the overall morphology of the hybrid thin film does not change much other than the approximate regular nanowall structure in Figure 5d. As can be seen from Figure 5e, large petal-like platelets in nanoscale grow vertically to the substrate. The accumulated small particles are enwrapped by these large petal-like platelets and thus partitioned by them to create a unique porous structure. Upon further increasing the concentration of MB (150 μM), no discernible and striking change in the morphology (Figure 5f) was observed except an increase in the porosity and thickness of the film.

Figure 6 shows the crystallographic orientation of the electrodeposited ZnO/MB hybrid thin films. The sharp diffraction peaks from XRD measurements have clearly proven that both pure ZnO and ZnO/MB hybrid films are well-crystallized.

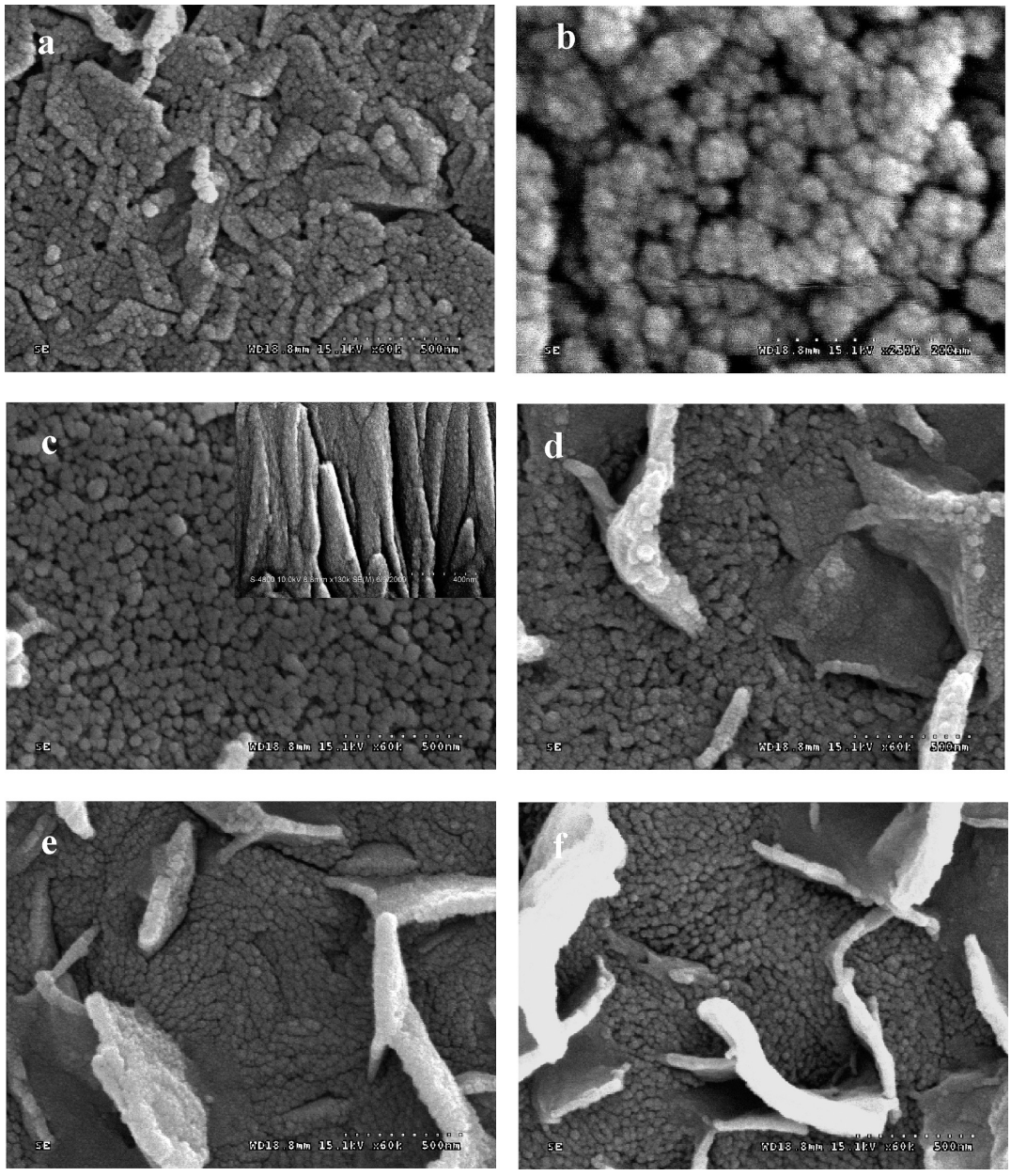

Figure 5. SEM images of the ZnO/MB hybrid thin films deposited with different MB concentrations of 9 (a, b), 30 (c), 60 (d), 120 (e), and 150 μM (f).

As expected, the XRD pattern of the pure ZnO film is in good agreement with the literature values (JCPDS card, no. 36-1451) except for some diffraction peaks from the FTO substrate. However, there is a sharp contrast of the relative peak intensities between the pure ZnO and ZnO/MB hybrid thin films. In comparison with the pure ZnO film, two ZnO/MB hybrid thin films exhibit dramatically increased intensities of the (100) and (101) diffraction, while the (002) peak becomes weaker. This phenomenon demonstrates that adsorption of MB molecules is preferentially onto the (002) plane of ZnO allowing the crystalline growth along the (100) or (101) plane,[7,18−20] but the concentration of dye added in the deposition solution has almost no effect on the crystallographic orientation of the deposited hybrid films.

As we know, ZnO is a good photocatalyst to degrade organic matter in water.[12,21,22] Since MB can be extracted absolutely from ZnO/MB hybrid films to form porous ZnO films, their photocatalytic activity was evaluated by using these porous films to photodegrade MB and EY. Before degradation, the blank

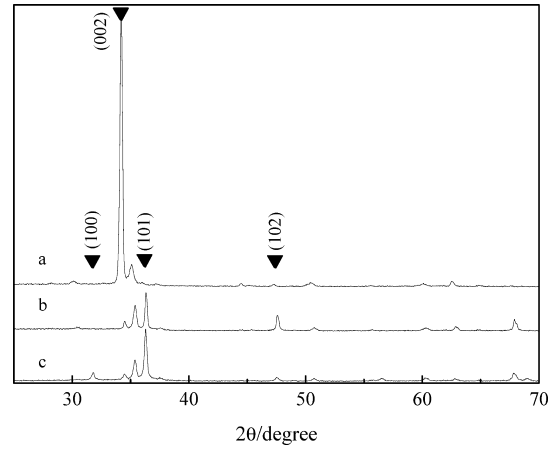

Figure 6. XRD patterns of the films electrodeposited at −1.0 V vs. SCE for 30 min from aqueous solutions of 5 mM $ZnCl_2$ without MB (a) and with MB of 90 μM (b) and 150 μM (c).

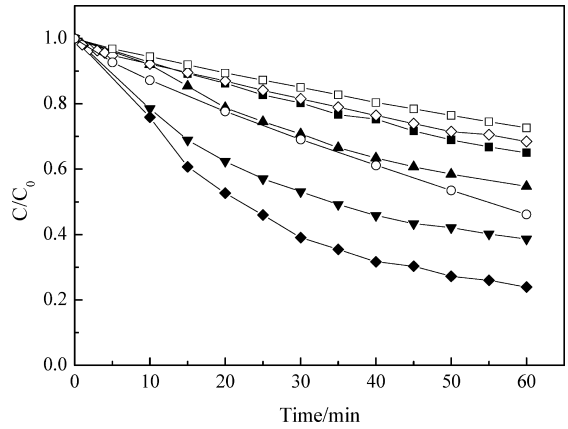

Figure 7. The photocatalytic degradation of EY (open symbol) and MB (solid symbol) by pure ZnO film (□, ■), porous ZnO films prepared by extracting dye from the ZnO/EY hybrid film deposited with 50 μM EY (○) and from the ZnO/MB hybrid film deposited with various MB concentrations of 60 (▲), 120 (▼), and 150 μM (◇, ◆).

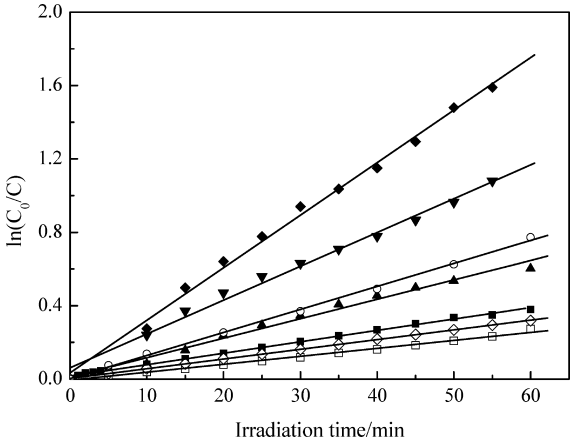

Figure 8. Relationship between irradiation time and $\ln(C_0/C)$ of photocatalytic degradation data shown in Figure 7.

experiment without photocatalyst was carried out to check the stability of MB and EY under irradiation of a high-pressure Hg lamp. Without ZnO films, the irradiated solution showed about 15% self-degradation within 60 min for MB and EY. This value was used to correct the following photodegradation results of ZnO films. A series of photocatalysis experiments were carried out with different substrates (MB and EY) and porous ZnO films. The remaining dye concentration as a function of irradiation time for these photocatalysis experiments is plotted in Figure 7. As a pure ZnO film was used as a photocatalyst, within 60 min, 35% of MB was degraded and 27% of EY was degraded. For a porous ZnO film prepared with the addition of 150 μM MB used as a catalyst, the degradation percentage is 76% for MB and 32% for EY, while for a porous ZnO film prepared with the addition of 50 μM EY, 54% of EY was degraded. Comparison of the degradation percentage of MB with that of EY under the same experimental condition indicates that porous ZnO films prepared by using MB as an additive are more efficient to degrade MB than EY. As already pointed out in the literature,[23,24] photocatalytic reactions of organic pollutants usually follow first-order kinetics. The kinetics of photodegradation reactions can be described by the Langmuir−Hinshelwood model by which the apparent rate constant can be determined. Figure 8 shows the linear relationship of $\ln(C_0/C)$ and irradiation time for the photocatalytic results as shown in Figure 7. The good linear relationship confirmed that all the photodegradation processes follow the first-order kinetics. The

TABLE 2: The Apparent Rate Constant of Photocatalytic Degradation by Different ZnO Films

	MB				EY	
additive[a]	none	60 μM MB	120 μM MB	150 μM MB	none	150 μM MB	50 μM EY
K/min^{-1}	0.0062	0.0106	0.0184	0.0286	0.0043	0.0053	0.0125

[a] The additive and added amount during electrodeposition of ZnO films.

photodegradation apparent rate constant for porous films prepared with various concentrations of MB, as listed in Table 2, is enhanced with the increasing addition content of MB during electrodeposition. This enhancement may be attributed to the more porous structure formed by adding a higher amount of MB. It is obvious that the photodegradation apparent rate constant for MB is almost 5.5 times higher than that of EY by the same porous film.

According to the literature,[24,25] the basic degradation mechanism can be explained as follows. Electron−hole pairs, generated by irradiating ZnO nanoparticles, can react with water to produce hydroxyl and superoxide radicals. These radicals can initiate a series of chemical reactions and act as a strong oxidizing agent to mineralize the pollutants. In our experiment, it is worth noticing that MB is used not only as a structure-directing agent during the electrodeposition of the hybrid film but also as a substrate to assess the photocatalytic performance of the electrodeposited porous film. Therefore, the special shape of holes, apertures, and surface morphology of ZnO generated by the addition of MB during electrodeposition makes the adsorption of MB much easier than that of EY. In other words, MB is capable of filling the self-tailored space subtly and exclusively, which is in agreement with the re-adsorption amount of MB and EY listed in Table 1. The photodegradation efficiency is drastically enhanced with the increase of dye concentration in the film. The big surface area and great adsorption ability of the hybrid film not only favor the interactions between film and dye, but also supply more active sites available for the generation of hydroxyl radicals.

4. Conclusions

ZnO/MB hybrid thin films with porous crystalline structures have been successfully fabricated on conductive FTO glass substrate from $ZnCl_2$ aqueous solution by using MB as a structure-directing agent. MB was found to effectively catalyze the growth of ZnO films and to significantly influence the film morphology. FTIR measurements suggest the formation of a chemical bond between the sulfonic groups and the ZnO surface. SEM morphologies of hybrid thin films show the irregularly connected nanoparticles 40 nm in diameter randomly stack and form narrow apertures as addition of 9 μM and 2D wall-like structures grow out of the plane and are randomly distributed on the surface layer of the film with further increasing MB concentration to 90 μM. XRD results demonstrate that adsorption of MB molecules is preferentially onto the (002) plane of ZnO allowing the crystalline growth along the (100) or (101) plane. The porous ZnO thin films prepared by extracting MB from ZnO/MB hybrid films show highly efficient photocatalytic activity. Furthermore, the photodegradation efficiency for the photodegradation of MB is higher than that of EY. This selective photodegradation to MB of ZnO films prepared with the addition of MB was attributed to the space generated after the extraction of MB from the hybrid film favoring the adsorption of MB much easier than EY. The felicitous and compact adsorption promotes

the photocatalytic selectivity. This is a very promising result of this study in view of the application of electrodeposited ZnO/dye hybrid films for the selective degradation of dye pollutants.

Acknowledgment. We gratefully acknowledge the financial support from the National Nature Science Foundation of China (20873162), the State Key Laboratory of Pollution Control and Resource Reuse Foundation (Nos. PCRRF09006 and PCRRF08009), and the Innovative Foundation of the Center for Molecular Science, Chinese Academy of Sciences (CMSCX200718). The authors are grateful to Prof. Yuan Lin for valuable discussions. Jingbo Zhang thanks Prof. Yoshida in Gifu University, Japan for his kind supervision in electrodeposition of ZnO/dye hybrid thin films.

References and Notes

(1) Yoshida, T.; Zhang, J. B.; Komatsu, D.; Sawatani, S.; Minoura, H.; Pauporte, T.; Lincot, D.; Oekermann, T.; Schlettwein, D.; Tada, H.; Wohrle, D.; Funabiki, K.; Matsui, M.; Miura, H.; Yanagi, H. *Adv. Funct. Mater.* **2009**, *19*, 17.

(2) Yoshida, T.; Komatsu, D.; Shimokawa, N.; Minoura, H. *Thin Solid Films* **2004**, *451*, 166.

(3) Fahoume, M.; Maghfoul, O.; Aggour, M.; Hartiti, B.; Chraibi, F.; Ennaoui, A. *Sol. Energy Mater. Sol. Cells* **2006**, *90*, 1437.

(4) Li, G. R.; Lu, X. H.; Qu, D. L.; Yao, C. Z.; Zheng, F. L.; Bu, Q.; Dawa, C. R.; Tong, Y. X. *J. Phys. Chem. C* **2007**, *111*, 6678.

(5) Sato, H.; Minami, T.; Miyata, T.; Takata, S.; Ishii, M. *Thin Solid Films* **1994**, *246*, 65.

(6) Martinez, M. A.; Herrero, J.; Gutierrez, M. T. *Sol. Energy Mater. Sol. Cells* **1997**, *45*, 75.

(7) Karuppuchamy, S.; Nonomura, K.; Yoshida, T.; Sugiura, T.; Minoura, H. *Solid State Ionics* **2002**, *151*, 19.

(8) Karuppuchamy, S.; Ito, S. *Vacuum* **2008**, *82*, 547.

(9) Xu, F.; Lu, Y. N.; Xie, Y.; Liu, Y. F. *Vacuum* **2008**, *83*, 360.

(10) Yoshida, T.; Terada, K.; Schlettwein, D.; Oekermann, T.; Sugiura, T.; Minoura, H. *Adv. Mater.* **2000**, *12*, 1214.

(11) Michaelis, E.; Wohrle, D.; Rathousky, J.; Wark, M. *Thin Solid Films* **2006**, *497*, 163.

(12) Pauporte, T.; Rathousky, J. *J. Phys. Chem. C* **2007**, *111*, 7639.

(13) Ichinose, K.; Yoshida, T. *Phys. Status Solidi A* **2008**, *205*, 2376.

(14) Boeckler, C.; Oekermann, T.; Saruban, M.; Ichinose, K.; Yoshida, T. *Phys. Status Solidi A* **2008**, *205*, 2388.

(15) Yoshida, T.; Pauporte, T.; Lincot, D.; Oekermann, T.; Minoura, H. *J. Electrochem. Soc.* **2003**, *150*, C608.

(16) Gan, X. Y.; Gao, X. D.; Qiu, J. J.; Li, X. M. *Appl. Surf. Sci.* **2008**, *254*, 3839.

(17) Pauporte, T.; Yoshida, T.; Cortes, R.; Froment, M.; Lincot, A. *J. Phys. Chem. B* **2003**, *107*, 10077.

(18) Yoshida, T.; Oekermann, T.; Okabe, K.; Schlettwein, D. *Electrochemistry* **2002**, *70*, 470.

(19) Yoshida, T.; Minoura, H. *Adv. Mater.* **2000**, *12*, 1219.

(20) Xu, L. F.; Guo, Y.; Liao, Q.; Zhang, J. P.; Xu, D. S. *J. Phys. Chem. B* **2005**, *109*, 13519.

(21) Qiu, R. L.; Zhang, D. D.; Mo, Y. Q.; Song, L.; Brewer, E.; Huang, X. F.; Xiong, Y. *J. Hazard. Mater.* **2008**, *156*, 80.

(22) Mai, F. D.; Chen, C. C.; Chen, J. L.; Liu, S. C. *J. Chromatogr., A* **2008**, *1189*, 355.

(23) Li, Y. Z.; Zhang, H.; Guo, Z. M.; Han, J. J.; Zhao, X. J.; Zhao, Q. N.; Kim, S. J. *Langmuir* **2008**, *24*, 8351.

(24) Li, X. Y.; Wang, D. S.; Cheng, G. X.; Luo, Q. Z.; An, J.; Wang, Y. H. *Appl. Catal. B* **2008**, *81*, 267.

(25) Chiou, C. H.; Wu, C. Y.; Juang, R. S. *Sep. Purif. Technol.* **2008**, *62*, 559.

JP903896J